



**Michigan  
Technological  
University**

Michigan Technological University  
**Digital Commons @ Michigan Tech**

---

Department of Geological and Mining  
Engineering and Sciences Publications

Department of Geological and Mining  
Engineering and Sciences

---

9-30-1984

## Amatitlan, An actively resurging cauldron 10 km south of Guatemala City

Richard L. Wunderman  
*Michigan Technological University*

William I. Rose  
*Michigan Technological University*

Follow this and additional works at: <https://digitalcommons.mtu.edu/geo-fp>

 Part of the [Geology Commons](#), [Mining Engineering Commons](#), and the [Other Engineering Commons](#)


---

### Recommended Citation

Wunderman, R. L., & Rose, W. I. (1984). Amatitlan, An actively resurging cauldron 10 km south of Guatemala City. *Journal of Geophysical Research*, 89(B10), 8525-8539. <http://dx.doi.org/10.1029/JB089iB10p08525>

Retrieved from: <https://digitalcommons.mtu.edu/geo-fp/137>

Follow this and additional works at: <https://digitalcommons.mtu.edu/geo-fp>

 Part of the [Geology Commons](#), [Mining Engineering Commons](#), and the [Other Engineering Commons](#)

AMATITLAN, AN ACTIVELY RESURGING CAULDRON 10 KM SOUTH OF GUATEMALA CITY

Richard L. Wunderman and William I. Rose

Dept. of Geol. and Geol. Engrg., Michigan Technological University

**Abstract.** A 14 x 16 km diameter collapse caldera has been recognized 10 km south of Guatemala City, Guatemala. The caldera is north of the presently active volcano Pacaya and west of Agua, a large stratovolcano. The caldera was not previously recognized because its eastern and western margins coincide with faults that outline the Guatemala City graben and because the northern margin of the caldera is buried by pyroclastic rocks. The existence of the northern caldera margin is now established by gravity data and a variety of geological observations including circumferential faults, hot springs, well-log data, and lithological changes in sedimentary rocks. A sequence of nine silicic pyroclastic deposits, totaling a volume of more than 70 km<sup>3</sup> of dense rock were erupted from the caldera. The ages of these eruptions are mainly between about 300,000 years B.P. to less than 23,000 years B.P. The rocks erupted at the caldera and its associated vents consist of domes and nonwelded pyroclastic flow, surge, and fall deposits, mainly of rhyolitic to dacitic composition. Successive pyroclastic eruptions have generally become smaller in volume and more silicic with time. Major and minor element chemistry distinguish Amatitlan pyroclastics from those of other nearby calderas. The caldera lies at the intersection of an offset of the volcanic chain (the Palin Shear) and the faults along the volcanic front (Jalpatagua fault zone). The caldera has a heavily faulted resurgent dome crosscut by an impressive longitudinal graben. The graben's alignment with the Jalpatagua fault zone suggests a genetic relationship. The longitudinal graben and resurgent dome are morphologically youthful and are the sites of many young silicic vents. Available seismic data show a heavy concentration of epicenters over the northern part of the resurgent dome, near a young silicic intrusion. The caldera is active and will probably erupt again. Over 1 million people live within 20 km and would be threatened in the event of a moderate eruption. Suggestions for future research focus on hazard assessment and forecasting.

Introduction

The Guatemalan Highlands lie on the continental side of a convergent plate boundary that trends north-northwest. Active subduction takes place in the Middle America Trench off the southwestern coast (Figure 1). The active "volcanic front" forms the southern border of the highlands [Carr, 1974]. The front rises from a coastal lowland and trends roughly parallel to the coast. Agua,

Pacaya, and other composite cones are part of this volcanic front, while Amatitlan and many other Central American silicic centers are north of the volcanic front [Rose et al., 1981].

The region south of Guatemala City (Figure 2) has been mapped at a scale of 1:50,000 by Eggers [1971, 1975] and Koch and McLean [1975]. These maps, together with work by Bonis et al. [1970], Williams [1960], Reynolds [1977, 1980], Brown et al. [1971], Carr et al. [1969], and Durgin et al. [1970], were used to make a geologic map (Figure 2). The extensive rhyolitic pyroclastic deposits of the area were described by Koch and McLean [1975], who concluded that these pyroclastics had their source region in the area south of Guatemala City. Eggers and Williams both concluded that the Amatitlan area was the site of a "volcano-tectonic depression."

Recently, important geophysical (gravity, seismic and electrical resistivity) and well-log data in the Amatitlan area were collected by Munoz et al. [1978]. Based on these earlier studies and on a variety of our field observations, we summarize the evidence that Amatitlan is a moderate-size caldera:

1. The arcuate depression around Lake Amatitlan is structurally and morphologically suggestive of a caldera. An arcuate scalloped topographic margin is visible on Landsat photos [Wunderman, 1983; Hahn, 1976], as well as numerous arcuate concentric normal faults (downward displacement toward the caldera's center) around the caldera's structural margin. Buried caldera faults on the floor of the Guatemala City Basin are revealed by geophysical techniques, and a 5-10 mgal gravity low is centered over the caldera [Munoz et al., 1978].

2. The presence of a caldera in the region is consistent with the large volumes of recent silicic pyroclastic rocks. Recognizing the source of the pyroclastics was south of, but not far from, Guatemala City, some earlier workers suggested that many of the pyroclastic flow and fall deposits were from Pacaya [Koch, 1970; McLean, 1970]. This is unlikely since it is now known that voluminous repeated eruptions of this type cause consequent surface collapse [Smith and Bailey, 1968]. No other appropriately sized depression is present nearby. We conclude that most of the voluminous silicic pyroclastics and domes were erupted from sources within the caldera.

3. A variety of other geologic features commonly observed in calderas is also present. These include present-day hot spring and fumarolic activity, surge deposits within the caldera, the mapped extent of lake sediments that follows (and helps delineate) the caldera's approximate northern extent, a breached caldera rim to the south, evidence of resurgence, and possible indications of continuing seismic activity within the caldera.

Copyright 1984 by the American Geophysical Union.

Paper number 4B0543.  
0148-0227/84/004B-0543\$05.00

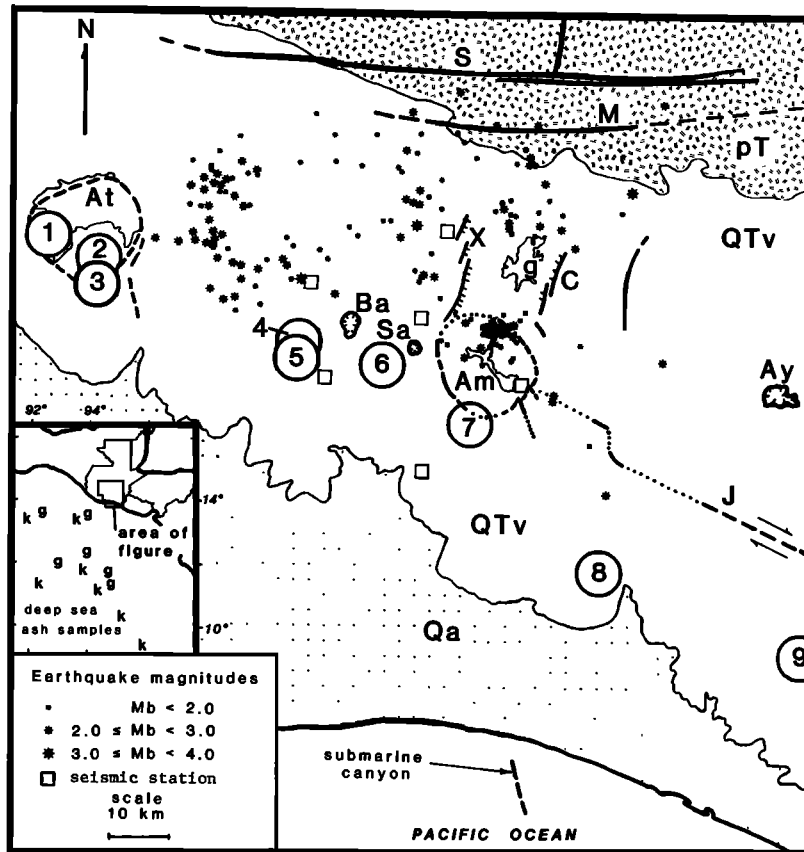


Fig. 1. Regional setting, structure, and seismicity of Amatitlan caldera. Inset is location map of Guatemala showing the area of the larger map. Letters in the Pacific Ocean denote deep-sea ash samples possibly correlative with Amatitlan units [Ledbetter, 1983]. The larger figure shows simplified geology of Guatemala with Quaternary alluvium (Qa), Quaternary and Tertiary volcanics (QTv), and pre-Tertiary rocks (pT). The volcanic front is composed of stratovolcanoes: (1) San Pedro, (2) Atitlan, (3) Toliman, (4) Actenango, (5) Fugeo, (6) Agua, (7) Pacaya, (8) Tecuamburro and (9) Moyuta. Slightly to the north of these stratovolcanoes are the silicic centers: At (Atitlan), Ba (Barahona), Sa (Sabana Grande), Am (Amatitlan), and Ay (Ayarza). Major faults include S (San Agustín), M (Motagua), and J (Jalpatagua), X (Mixco), and C (Santa Catarina Pinula). Earthquake epicenters for May 1976 from White and Harlow [1979] are shown to demonstrate the clustering of epicenters that have occurred at and around the caldera during all of the recent years. Guatemala City is located at the letter g.

### Stratigraphy

#### Older Precaldera Rocks (Tu)

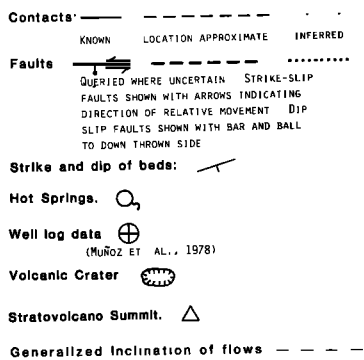
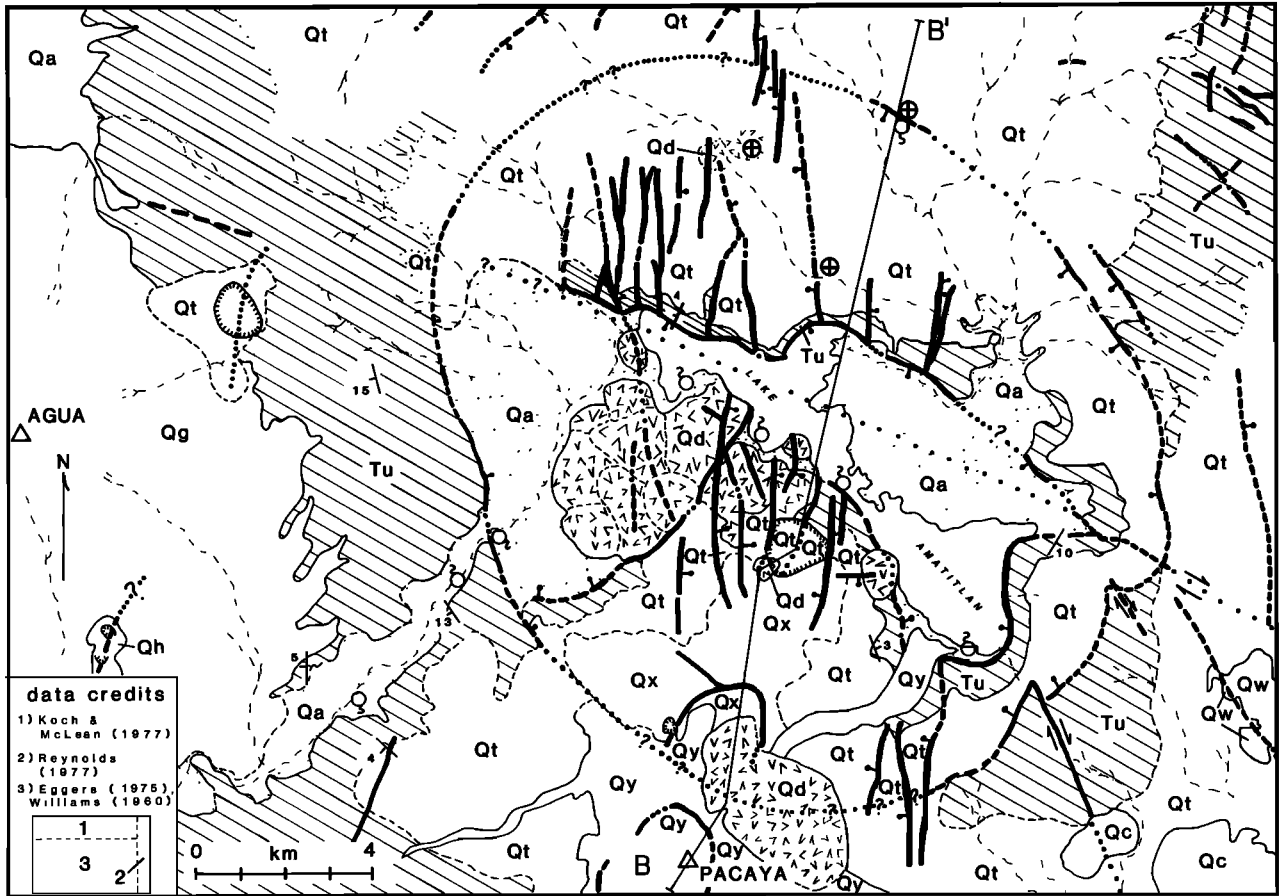
Older rocks preserved in and around the caldera are Cretaceous(?) granite, and various Tertiary volcanic rocks (Figure 2). The volcanics include laharic units and andesitic flows, and dip westward on the western side of the caldera. On the caldera's east side the Tertiary units dip to the east [Eggers, 1971]. The data together suggest that a Tertiary volcano may have been centered in the caldera region before collapse.

#### Surficial Pumiceous Deposits

Silicic pyroclastic rocks (Qt). Nomenclature of individual surficial pumiceous units (Figure 3) follows that proposed by Koch and McLean [1975]. Wunderman [1983] presents lithic size isopleths, as well as more detailed isopach maps for the pyroclastic deposits discussed here. These young

silicic pyroclastic rocks are pumiceous fall deposits interbedded in basins with pumiceous pyroclastic flows. All of the deposits are nonwelded to slightly welded. They are generally rhyolitic in the broad sense, ranging from 66 to 76% SiO<sub>2</sub> and show calc-alkalic affinities. Outside of the topographic basins pyroclastic flow units are generally absent. Within the basins the deposits are sometimes more than 100 m thick and develop steep cliff faces along stream valleys. The distribution of individual surficial pumiceous units are collectively designated Qt in Figure 2. Table 1 presents some general characteristics of the silicic pyroclastics from Amatitlan. In some units at Amatitlan a minor (0-2%) basaltic to andesitic component is present. The mafic component is in the form of basaltic blebs, either dense or scoriaceous, and as banded pumice clasts that show varying degrees of mixing with the host rhyolite.

Dominant phenocrysts in the Amatitlan pyroclastics are plagioclase and sparse quartz.



**Quaternary Surficial Deposits**

**Qa Alluvium and Colluvium** MAPPED WHERE NOT COVERED BY PYROCLASTIC FALLS AND FLOWS

**Quaternary Intermediate to Mafic Volcanics**

**Qc Cinder Cones** BASALTIC SCORIA ASHFALL AND ASSOCIATED BASALT FLOWS.

**Qy Basalt Flows of Pacaya** INCLUDES THE "HISTORIC", "MODERN" AND "INITIAL" GROUPINGS OF EGERS (1970)

**Qx Ancestral Pacaya** PYROXENE ANDESITE LAVAS.

**Qw Andesite and Basalt Flows**

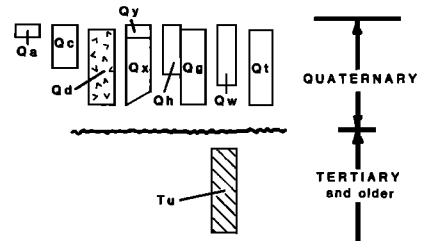
**Qg Andesite Flows of Agua**

**Qh Parasitic Cinder Cones** BASALTIC SCORIA ASHFALL DEPOSITS INTERBEDDED WITH OLIVINE BASALTIC ANDESITE LAVAS, ON AGUA'S FLANKS.

**Quaternary Silicic to Intermediate Volcanics**

**Qd Domes** RHYOLITE TO ANDESITE DOMES AND FLOWS.

**Qt Silicic Pyroclastics** NON-WELDED FLOW AND FALL DEPOSITS, INTERBEDDED BRECCIAS, SOILS, ALLUVIUM AND OCCASIONAL LAKE AND STREAM SEDIMENTS.



**Tertiary and Older Volcanics**

**Tu** UNDIFFERENTIATED PRE-CALDERA UNITS BASALT AND ANDESITE FLOWS, SILICIC LAVAS, PYROCLASTIC ROCKS, LAHARS, AND UNDATED DIORITES AND GRANITES.

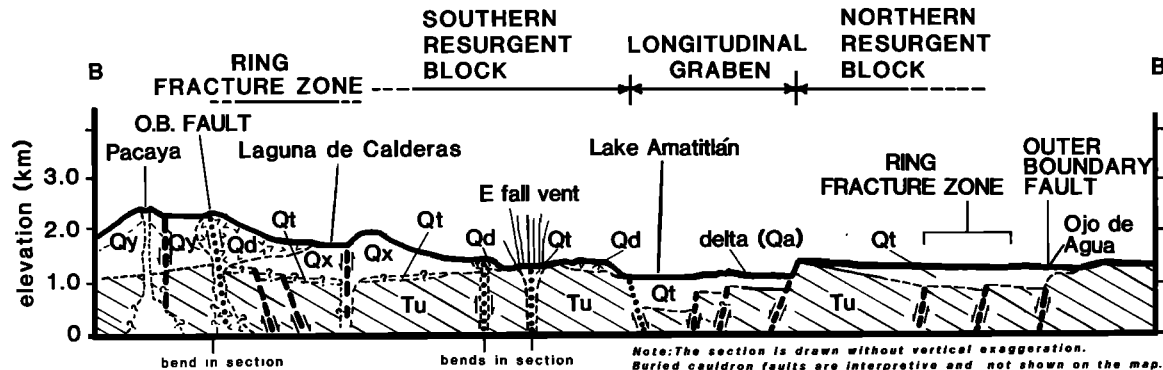


Fig. 2. Generalized geologic map of Amatitlan caldera with descriptions of map units, key, and cross section in the continued part of the figure. The map is based on a more detailed 1:50,000 scale map compiled by Wunderman [1983].

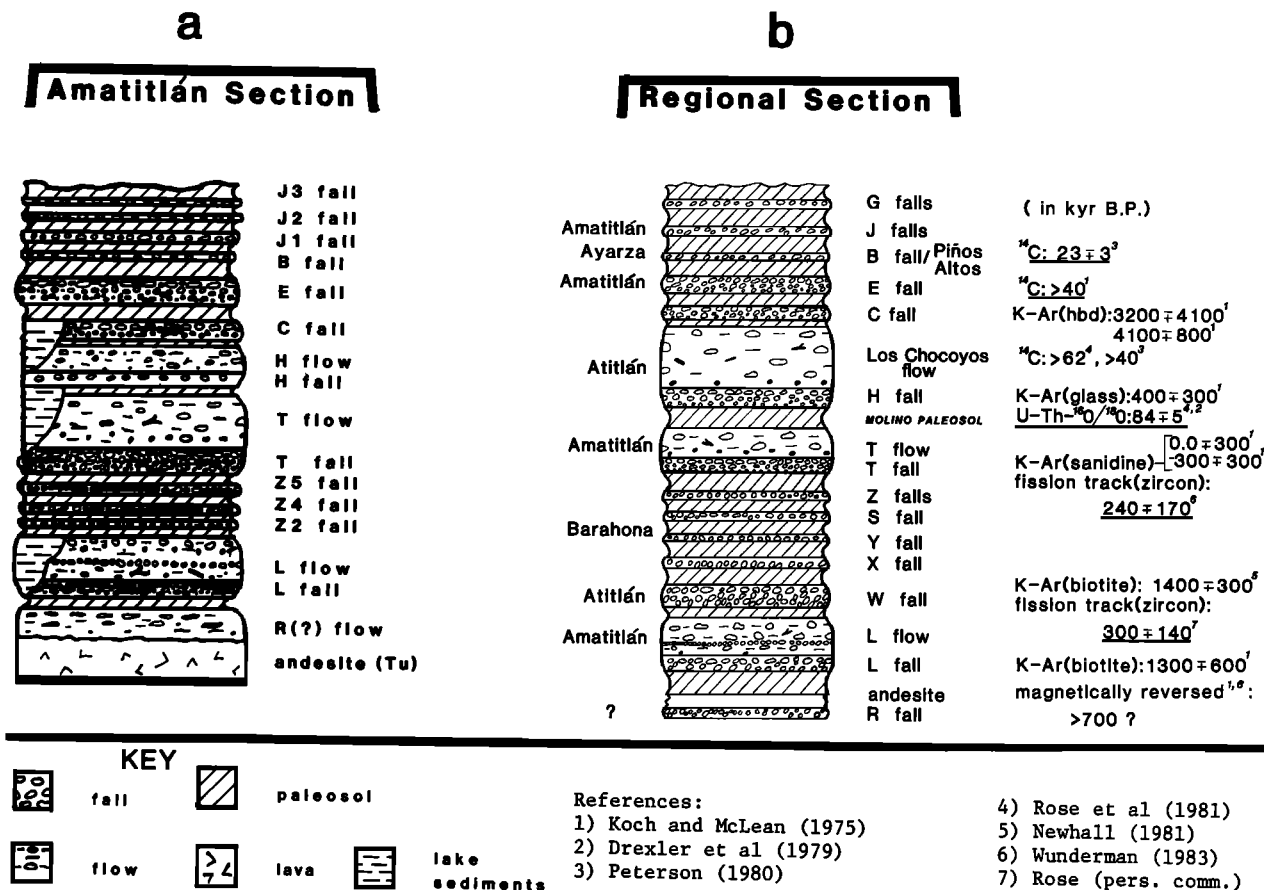


Fig. 3. Stratigraphic relations, nomenclature, source vent areas, and age determinations of surficial silicic pyroclasts. (a) Stratigraphic relations compiled in the vicinity of Amatitlan. (b) Regional stratigraphic relations compiled between Ayarza and Atitlan and age determinations with references, preferred ages underlined. The Molino paleosol divides the section into the older Sumpango group and younger San Cristobal group.

Sanidine is absent or rare. Mafic minerals are typically hornblende and biotite (sometimes one without the other), Fe-Ti oxides, and hypersthene [Koch, 1970; McLean, 1970]. Occasional phenocrysts of zircon and microlites of apatite occur. Hypersthene is the dominant mafic phenocryst in only one minor ash (Z5 fall).

**R flow and fall deposits.** R fall consists of three airfall deposits named R1, R2, and R3 (young to old, Figure 3) by McLean [1970]. These three falls are stratigraphically beneath the R flow and are not necessarily genetically related to each other or to the R flow. The R fall is recognized at only a few scattered sites in the central volcanic highlands from Patzicia to Guatemala City. Reversed magnetic polarity (first recognized by Koch and McLean [1975]) for andesite overlying R1 fall at km 23, Highway CA-1 was reconfirmed by examining oriented samples. This indicates that R units may be older than the last magnetic reversal, about 700,000 years B.P.

The name R flow was used by McLean [1970] for the oldest pyroclastic flows in the Guatemala City area. It is infrequently exposed and has not been studied in detail. The R flow is well exposed in an 80 m deep barranca at La Florida, 3.2 km northwest of Guatemala City [Koch and McLean, 1975; Figure 11]. R overlies some Tertiary andesite flows shown as Tu (Figure 3a) at the

north shore of Lake Amatitlan. R pumices are considerably more weathered in their appearance than the overlying sequence of young pyroclastic units, suggesting that the R flow may be much older than overlying pyroclastic deposits. We suggest that the R flow may represent several different eruptive units, based on its variable appearance in outcrop.

**Quaternary Deposits**

**L fall and flow.** The L fall and flow deposits overlie sediments derived partly from R (Figure 3). The L fall and the two subsequent L flow members (L1, L2) were each deposited one on top of another without a cooling break [Koch and McLean, 1975; Wunderman, 1983]. L fall is widely distributed between Guatemala City and Lake Atitlan (Figure 4). Chemical fingerprinting of previously identified ashes to the east of Guatemala City indicates that L fall is present in substantial amounts there also. Toward Amatitlan, L fall thickens to over 10 m. L fall is very well exposed in road cuts along CA-9 and in barrancas between Amatitlan and Guatemala City.

The L fall deposit is divided into three parts by persistent fine-grained beds of crystal-rich ash that occur near the middle of the deposit. These continuous 2-10 cm thick beds are absent in

TABLE 1. Features of Silicic Pyroclastic Units From Amatitlan Cauldron and Vicinity

| Unit    | Major Fe-Mg Phenocrysts | Pumice Color            | Thickness, m | Maximum Location              | Minimum Areal Distribution, km <sup>2</sup> |
|---------|-------------------------|-------------------------|--------------|-------------------------------|---|
| J3 fall | bio                     | white                   | 0.4          | km 33, Hwy. CA-9              | 130   |
| J2 fall | bio, cpx                | white                   | 0.4          | km 33, Hwy. CA-9              | 130   |
| J1 fall | hbl, bio                | white                   | 2.0          | Laguna de Calderas            | 110   |
| E fall  | hbl, hyp, bio           | white                   | 10.0         | N. of Lake Amatitlan          | 1300  |
| C fall  | hbl                     | white                   | 4.6          | km 23, Hwy. CA-9<br>Amatitlan | 1000  |
| T flow  | hbl, bio                | very<br>lt. gray        | -            | Guatemala City<br>Basin       |   |
| T fall  | hbl, bio                | white                   | 5.0          | km 24, Hwy. CA-9<br>Amatitlan | 2600  |
| Z5 fall | hyp                     | white                   | 3.0          | U.N. Park, Amatitlan          | 200   |
| Z4 fall | hbl, bio                | white                   | 1.0          | U.N. Park, Amatitlan          | 500   |
| Z2 fall | hbl                     | lt. gray                | 2.0          | U.N. Park, Amatitlan          | 200   |
| L flow  | bio, hbl                | pale<br>brown           | -            | Guatemala City<br>Basin       |   |
| L       | hbl, bio                | lt.<br>brown to<br>gray | 10.0         | Guatemala City<br>Basin       | 1600  |

After Koch and McLean [1975]; bio, biotite; cpx, clinopyroxene; hbl, hornblende; hyp, hypersthene.

other deposits of the region. Between the fine beds, the fall materials are reversely graded.

Mafic lithic fragments in the L fall increase in number and size approaching the caldera. The L fall deposit contains loose fragments of mafic cauliflower-like basalt blebs that are interpreted as minor mafic magma quenched against the rhyolitic host. L fall pumices are light brownish gray to white in color.

The L1 flow member's thickness is usually less than 50 m, and it is well exposed in many Guatemala City Basin barrancas. The member also forms a substantial part of the extensive surficial pyroclastic deposits from Amatitlan, east of the Guatemala City Basin [Wunderman, 1983]. The L2 member is restricted to drainages west of the Guatemala City Basin and is usually less than 30 m thick. The contact of the two ash flows is often conformable, and no accumulation of soil is ever present between the flows. For this reason the two L ash flows are believed to be two lobes produced during the same eruption.

Flat-lying sediments of lacustrine and fluvial origin overlie the L flows and occur below about 1600 m elevation in deep barrancas throughout the Guatemala City Basin. Fluvial sediments are poorly sorted and display both cross and graded bedding. Lacustrine sequences contain thin bedded chalky white diatomaceous mudstone and interbedded pumice and basaltic scoria -- often up to 2 m thick (see below).

**Z Falls.** McLean [1970] named and recognized five minor falls, the Z falls (Figure 3b). The Z2, Z4, and Z5 falls (old to young) are thickest in the Amatitlan vicinity (Figure 3a) and all best

exposed at U.N. Park. Z2 has only been recognized at U.N. Park. It is 0.25 m thick, contains lapilli-sized pumices and is devoid of lithics. The pumices are light gray in color and often mixed in this unit. The dominant mafic phenocryst is hornblende (Table 2). Chemistry and correlation data of Z2 suggest that it is unrelated to the Amatitlan falls and that it is much like the C fall, which was erupted from an extra-caldera source (see below).

The distribution of Z4 is considerably wider than the Z2 or Z5 falls (Figure 4). Near Lake Amatitlan maximum mean lithic sizes increase to over 4 cm in diameter [Wunderman, 1983], indicating proximity to source. Pumices from Z4's basalt section are unusually dense and include gray, mafic swirls. Hornblende is the dominant mafic phenocryst. Z4 overlies Z2, the two being separated by a paleosol at U.N. Park.

The Z5 airfall is found only near the caldera (Figure 4). Z5 is a reversely graded unit with a fine-grained 0.5 m thick basal portion. Above the fine-grained zone the unit is layered, poorly-sorted, and lithic rich. Green hypersthene is the dominant mafic mineral.

**T fall and flow.** Stratigraphically T fall and flow overlie Z5 fall and an intervening paleosol and underlie the very distinctive Los Chocoyos deposits and an intervening paleosol. T flow is the youngest flow from Amatitlan cauldron and overlies T fall without a cooling break (Figure 3).

T fall is visible in many road cuts and natural exposures near Amatitlan. Dispersal (Figure 4) is wider than any other fall in the region except H.

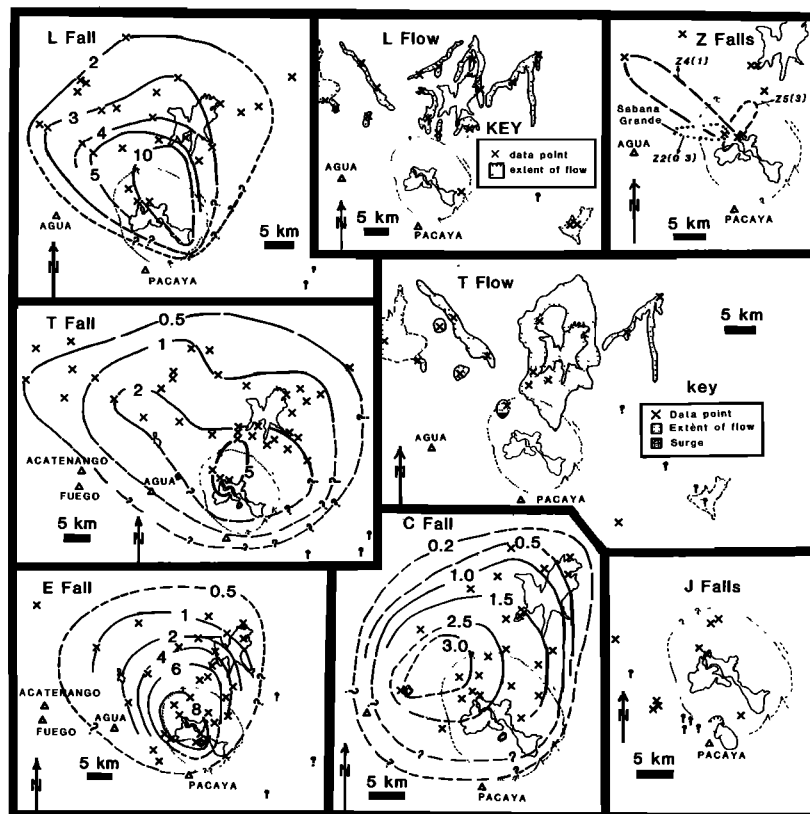


Fig. 4. Isopach maps of pyroclastic deposits of Amatitlan modified from Koch [1970] and McLean [1970]. Refinements on their data were made in the near-source areas and in tracing Amatitlan units to the east by using chemical fingerprinting [Wunderman, 1983]. Locations of data points are shown by crosses, and isopach units are in meters. Locations where an Amatitlan source is indicated by chemical fingerprinting, but the specific unit is less clear, are shown by question marks (see text). The isopach data are dependent on preservation and exposure, and thus we expect the actual distribution of units to be greater than shown. Some of the larger units such as L and T could be preserved as deep-sea ash layers such as those on Figure 1, inset.

Maximum thickness is 5 m, seen near the northern edge of the caldera, where it is generally very lithic-rich.

T flow's thickness exceeds 100 m in some deep barrancas in the Guatemala City Basin, although it generally is tens of meters thick. T flow is characterized by incorporation of large amounts of carbonized debris and the prominence of proximal lithic lag breccias. In some exposures near Amatitlan, lithic fragments make up 40-70% of T flow's volume, in contrast to lithic contents of less than 20% in L, T, and R ash flows, and less than 10% in the distal Los Chocoyos flow deposits [Koch and McLean, 1975]. The T flow deposit contains complicated surge stratification at one exposure in the cauldron consisting of a thickness of interbedded sand wave and planar beds. The deposit is fine grained and sometimes appears texturally similar to siltstone [Wunderman, 1983].

**C fall.** The C fall is a conspicuous unit in the vicinity of the caldera and is also widely distributed in the Guatemala City area and surrounding highlands (Figure 4 [after Koch, 1970]). The fall has a characteristic granular, well-sorted appearance and contains a distinctive white, relatively dense hornblende-bearing pumice. Within the boundaries of an inferred ancestral crater lake (see below), C fall is interbedded

with lake sediments and shows stratification and reverse grading consistent with deposition in water. Outside of this lacustrine environment but within basins, C lies upon sediments or the intervening paleosol and top of the Los Chocoyos flow deposit. In highlands where Los Chocoyos flow deposition is lacking, C is above the intervening paleosol and the H fall deposit.

**E fall.** The distribution of E fall deposits is among the best known, since as a voluminous recent fall in the Amatitlan Cauldron area it is often very near the surface (Figure 4). The E fall is coarse grained and everywhere conspicuously reversely graded. Layer E's maximum thickness is 10 m at the north side of Lake Amatitlan. Near

TABLE 2. Zircon Fission Track Age of T-Fall Deposit

|                                |   |
|--------------------------------|---|
| Sample no.                     | 9-T, DF 1674                            |
| No. of grains studied          | 8                                       |
| No. of fossil tracks           | 8                                       |
| No. of induced detector tracks | 1080                                    |
| Neutron flux                   | $1.07 \times 10^{15}$ n/cm <sup>2</sup> |
| Calculated age                 | 0.25 Ma B.P.                            |
| 2 sigma uncertainty            | $\pm 0.17$                              |

Villa Nueva, pumice bombs in E are up to 23 cm in diameter and lithic fragments just south of Guatemala City are as coarse as 1.5 cm in diameter [Koch, 1970]. Lithic fragments comprise only 1-2% [Koch, 1970] and are of varied composition. E pumices contain hornblende, biotite, and hypersthene phenocrysts, with increasing hypersthene and decreasing biotite up from the base of the layer [Koch, 1970]. Despite this, E fall's whole-rock chemistry is surprisingly constant (see below).

**J falls.** Koch [1970] named the J1, J2, and J3 fall deposits (old to young), the most recent pyroclastic products of Amatitlan. The distribution and thickness of the three J fall deposits is much less than most Amatitlan fall deposits (Figure 4). Generally the J falls occur within a meter of the surface. The three layers are best exposed together at kilometer 33 on Highway CA-9 south of Amatitlan.

#### Quaternary Domes and Flows (Qd)

Domes and viscous flows in Amatitlan Quadrangle were mapped by Eggers [1971], who divided them into two groups based on composition. One group includes latite-andesites and dacites, the second group is rhyolitic. Domes are most abundant in the southwestern part of the central cauldron beside the lake, but very large domes occur near Pacaya as well. The domes are exogenous and steep sided.

Dome rocks are glassy (perlitic and spherulitic), sometimes vesicular, and consistently contain phenocrysts of plagioclase. In the more mafic samples the phenocryst content increases. The more silicic units have biotite, oxyhornblende, plagioclase (An 20 to An 40) phenocrysts, while more mafic domes have augite, hypersthene, plagioclase (An 35 to An 60), and Fe-Ti oxides [Eggers, 1971].

The age of most of the domes and flows is not precisely known, but based on the depth of pyroclastic cover, many of them postdate the largest (L and T) fall deposits. One dome near Villa Nueva penetrates the C fall, and appears to deform (and therefore postdate) the E fall.

In addition to the domes a series of pyroxene andesite lavas form a cone that covers a considerable portion of the southern quadrant of Amatitlan caldera (Qx, Figure 2). Phenocryst content of the lavas is plagioclase (An 37-74) augite, hypersthene, rare olivine, and opaques [Eggers, 1971]. The cone, called "ancestral Pacaya" by Eggers, contains an impressive south-facing V-shaped crater located about 4 km north of Pacaya's summit. The crater floor is partly covered by a small lake called Laguna de Calderas. Rocks from "ancestral Pacaya" have not been dated.

#### Age of Amatitlan's Pyroclastics

Dating Guatemalan silicic ash eruptions has been a challenge because the rocks often lack sanidine, are too young to be dated very accurately by K-Ar methods, and are mostly too old to be dated by carbon-14 study of incorporated charcoal fragments. Major contributions to establishing a chronology for these eruptions were made by Koch [1970] and McLean [1970], who

elaborated the first stratigraphic synthesis of the silicic fall and flow deposits, and by Drexler et al. [1980] who established the age of the Los Chocoyos pyroclastic deposit, the largest single Quaternary silicic unit in Guatemala (Figure 3).

Table 2 shows results of new fission track study of zircon from the T fall deposits, giving an age of 0.24 +/- 0.17 Ma. Figure 3 is a compilation of known age determinations on Quaternary tephra in Guatemala.

K-Ar dates on hornblende, glass, and biotite give ages that are older than the fission track ages. The K-Ar ages, particularly on some deposits (e.g., C) are clearly unreasonable. The fission track ages are believed to be more reliable.

#### Paleosols and Lake Sediments

Where sections through the Amatitlan pyroclastics are undisturbed by erosion, regionally continuous paleosols have formed. Surrounding Lake Amatitlan, however, the continuity of paleosols is notably broken, and horizons occupied by paleosols elsewhere are instead characterized by lacustrine sediments [Koch, 1970; McLean, 1970; Munoz et al., 1978]. These are "composed of white, very well-bedded, tuffaceous, diatomaceous mudstones interbedded with a few thin cinder layers and thin black carbonaceous laminae" [Koch, 1970]. They are usually found below 1600 m in elevation. At about 1600 m and higher elevations, surrounding the area of lacustrine sediments, fluvial deposits of pumiceous conglomerate, sandstone, and mudstone are found at the same horizons.

The distribution of such deposits can be well delineated in the area north of present-day Lake Amatitlan (Figure 5). Stratigraphically such deposits occur above the L unit and both above and below the T, H and C units (Figure 3b). The distribution of such materials shows that a large lake occupied much of the Amatitlan caldera following the eruptions of the L pyroclastics (Figure 5). Since such sediments are not found immediately above or below the E fall deposit, the lake must have receded by this time. This recession is thought to be related to the breaching of the southern caldera wall, probably by the Rio Michatoya.

The distribution of the sediments from the ancestral Amatitlan caldera lake is unknown in the region to the south, where younger volcanic rocks have buried these horizons. It is noteworthy that highly silicic xenoliths seen in Pacaya's recent lavas [Rose, 1967; Eggers, 1971] may be fused diatomaceous material. However, the xenoliths are inconclusive evidence for caldera lake sediments beneath Pacaya, as diatomaceous sediments are also common in the precaldra rocks. Thus there is strong evidence for a much larger Lake Amatitlan that occupied at least the northern half of the caldera for the period between the L and C eruptions and which drained, possibly due to resurgence, prior to the E eruption.

#### Geochemistry of Amatitlan Volcanic Rocks

Whole-rock samples of all of the pyroclastic units from Amatitlan were analyzed using X-ray fluorescence (XRF) and INAA methods. Average



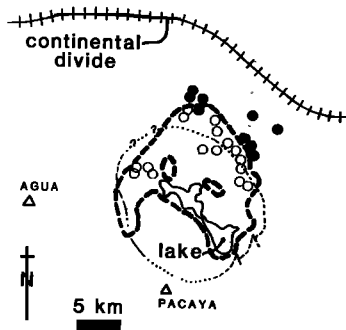


Fig. 5. Distribution of lacustrine and fluvial sediments interbedded with Quaternary silicic pyroclastics. A compilation of the distribution of lacustrine and fluvial sediments (open and solid circles, respectively) in the southern Guatemala City Basin [after Munoz et al., 1978]. The sediments shown are post-L to pre-E in age. The heavy dashed line is the approximate average extent of a former Lake Amatitlan that Koch [1970] and McLean [1970] recognized. The two small areas shown as elliptical circles just north of the present-day lake were probably highs, partly or completely caused by resurgence (see text). The former lake's southern edge is influenced by extrusive silicic domes that deny exposure of underlying rocks. Location of the continental divide upslope from the caldera in the Guatemala City Basin helps explain why the northern margin is covered with thick fill. Present-day topography acts to funnel material toward the caldera.

compositions for the Amatitlan pyroclastic units (in stratigraphic order) are given in Table 3. Although each unit has some variability of composition that is not shown by the averaging, the averages describe compositions of calc-alkalic dacites and rhyolites. There is a weak but systematic chemical variation with time:  $\text{SiO}_2$ , Cs, and Rb generally increase,  $\text{Fe}_2\text{O}_3$ , MgO, CaO,  $\text{TiO}_2$ ,  $\text{P}_2\text{O}_5$ , Ba, Ce, Co, Eu, Hf, La, Lu, Nd, Sc, Sm, Sr, Tb, Yb, and Zr decrease (Table 3, Figure 6). The Amatitlan pyroclastics are chemically distinct from the pyroclastics from other Central American silicic centers (Figure 7). The trend of variation shown by the Amatitlan pyroclastics is the same as the chemical variation pattern of the domes within the Amatitlan area, based on the work of Eggers [1971, Figure 8]. In fact, the apparent "gap" in composition shown by the domes (Figure 8) is filled by the pyroclastic rocks. From this we agree with Eggers that the dome rocks and the pyroclastics are part of a single, related calc-alkalic group of magmas. The chemical/time trends that apply to the pyroclastic rocks (Figure 6) can possibly be applied to the domes in order to clarify their eruption sequence [Wunderman, 1983].

Ashes erupted from the same source at different times have more chemical similarity than ashes erupted from separate sources [Sarna-Wojcicki et al., 1979; Peterson, 1980]. Sarna-Wojcicki et al. [1979] used a statistical value, the coefficient of similarity (CS), to quantify the chemical similarity of volcanic ashes. CS values for "known" Amatitlan ashes compared with each other average  $0.83 \pm 0.06$ . Generally, CS comparisons

yield highest values for units that are stratigraphically close to each other. When compared with rhyolitic ashes from other volcanoes, the Amatitlan ashes exhibit CS values ranging between 0.50 and 0.80, and averaging  $0.69 \pm 0.07$  (Table 4).

The geochemical data on C and Z3 fall deposits are given in Table 5. These units are compositionally similar to each other but do not appear to be part of the Amatitlan suite. When compared to Amatitlan units, the mean CS for C fall and Z2 fall are both  $0.64 \pm 0.04$ , lower than any inter-Amatitlan comparisons. Thus the geochemical data support the interpretation of C and Z2 as extra-caldera fall deposits. The distribution of C is consistent with a source at Sabana Grande, northeast of Agua (Figure 4). If it is the source, Sabana Grande is another example of an obscurely expressed silicic vent area. Eggers [1971] interprets it to be the head of a valley cut in Tertiary rocks, whose lower course has been filled and covered with mudflows and lava flows from Agua. Field data on Z2 are inadequate, but the high degree of chemical similarity between C and Z2 (CS = 0.81) suggests they could be related to the same parent magma body.

#### Distributions of Eruptive Units

The extensive field data of Koch and McLean [1975] were supplemented by new observations to derive the maps shown in Figure 4. In general the location of greatest isopach thickness is a rough estimate of source, but it is best used in conjunction with grain size distribution [Walker, 1980]. Koch and McLean [1975] concluded that Agua and Pacaya were vents for the Amatitlan pyroclastics. This is volcanologically unlikely because the eruption of such large volumes of material is typically accompanied by collapse. We

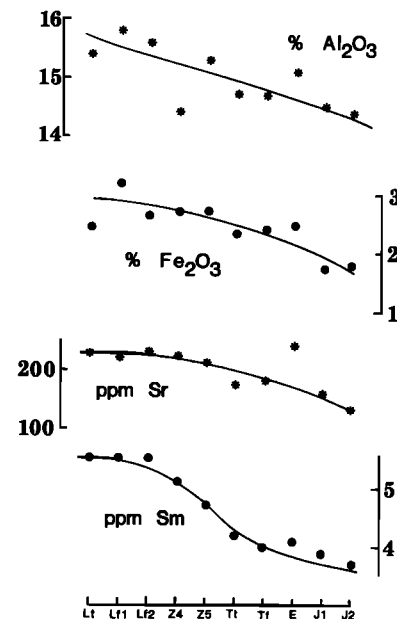


Fig. 6. Change of chemical composition of Amatitlan pyroclastic rocks with time. Stratigraphic order from oldest (Lt) to youngest (J2). Data from Table 3.

TABLE 3. Average Composition of Amatitlan Rhyolitic Pyroclastic Units

| Unit                             | wt. %       |           |          |           |           |           |           |              |              |           |
|----------------------------------|-------------|-----------|----------|-----------|-----------|-----------|-----------|--------------|--------------|-----------|
|                                  | J2<br>(1)** | J1<br>(1) | E<br>(4) | Tf<br>(4) | Tt<br>(3) | Z5<br>(2) | Z4<br>(2) | Lf(2)<br>(5) | Lf(1)<br>(3) | Lt<br>(4) |
| SiO <sub>2</sub>                 | 73.8        | 74.7      | 71.0     | 70.1      | 69.8      | 72.0      | 68.2      | 70.7         | 69.2         | 70.8      |
| Al <sub>2</sub> O <sub>3</sub>   | 14.4        | 14.5      | 15.1     | 14.7      | 14.7      | 15.3      | 14.4      | 15.6         | 15.8         | 15.4      |
| Fe <sub>2</sub> O <sub>3</sub> * | 1.80        | 1.73      | 2.50     | 2.40      | 2.35      | 2.71      | 2.70      | 2.63         | 3.20         | 2.41      |
| MgO                              | 0.33        | 0.31      | 0.55     | 0.51      | 0.51      | 0.48      | 0.55      | 0.66         | 0.80         | 0.54      |
| CaO                              | 1.1         | 1.1       | 1.9      | 1.5       | 1.5       | 1.8       | 1.8       | 1.8          | 2.1          | 1.2       |
| Na <sub>2</sub> O                | 4.00        | 4.40      | 4.20     | 4.00      | 4.02      | 4.25      | 3.90      | 4.17         | 4.10         | 3.95      |
| K <sub>2</sub> O                 | 4.10        | 4.00      | 3.90     | 4.20      | 4.00      | 3.90      | 2.90      | 4.15         | 3.80         | 4.22      |
| TiO <sub>2</sub>                 | 0.32        | 0.31      | 0.42     | 0.39      | 0.38      | 0.42      | 0.42      | 0.52         | 0.49         | 0.46      |
| P <sub>2</sub> O <sub>5</sub>    | 0.04        | 0.04      | 0.07     | 0.06      | 0.06      | 0.06      | 0.07      | 0.07         | 0.07         | 0.06      |
|                                  | ppm         |           |          |           |           |           |           |              |              |           |
| Sc                               | 2           | 2         | 4        | 3         | 3         | 5         | 4         | 4            | 6            | 4         |
| Co                               | 1.3         | 0.8       | 3.1      | 2.7       | 2.8       | 3.1       | 2.9       | 3.4          | 1.3          | 2.0       |
| Rb                               | 115         | 118       | 102      | 100       | 105       | 95        | 96        | 99           | 100          | 105       |
| Sr                               | 136         | 160       | 242      | 183       | 175       | 213       | 226       | 231          | 227          | 229       |
| Y                                | 11          | 13        | 12       | 12        | 12        | 11        | 14        | 13           | 12           | 15        |
| Zr                               | 228         | 232       | 247      | 242       | 251       | 281       | 284       | 300          | 249          | 311       |
| Cs                               | 3.3         | 3.4       | 2.8      | 3.2       | 3.3       | 3.1       | 3.1       | 2.8          | 3.0          | 3.0       |
| Ba                               | 1287        | 1323      | 1270     | 1342      | 1331      | 1368      | 1316      | 1369         | 1267         | 1367      |
| La                               | 27          | 22        | 24       | 27        | 24        | 26        | 25        | 31           | 26           | 29        |
| Ce                               | 47          | 52        | 52       | 52        | 52        | 59        | 64        | 57           | 58           | 62        |
| Nd                               | 18          | 18        | 20       | 20        | 21        | 17        | 31        | 27           | 39           | 26        |
| Sm                               | 3.7         | 3.9       | 4.1      | 4.0       | 4.2       | 4.7       | 5.1       | 5.5          | 5.5          | 5.5       |
| Eu                               | 0.78        | 0.80      | 1.05     | 0.88      | 0.99      | 1.00      | 1.05      | 1.30         | 1.30         | 1.30      |
| Tb                               | 0.59        | 0.60      | 0.70     | 0.67      | 0.74      | 0.77      | 0.92      | 1.00         | 0.87         | 0.92      |
| Yb                               | 1.8         | 1.9       | 2.0      | 1.9       | 2.0       | 2.2       | 2.4       | 2.5          | 2.4          | 2.6       |
| Lu                               | 0.29        | 0.29      | 0.30     | 0.31      | 0.32      | 0.32      | 0.39      | 0.35         | 0.35         | 0.40      |
| Hf                               | 6.0         | 6.0       | 7.0      | 6.2       | 6.4       | 7.0       | 8.0       | 7.4          | 7.8          | 7.9       |
| Pb                               | 16          | 14        | 12       | 12        | 15        | 20        | 8         | 14           | 19           | 15        |
| Th                               | 9.3         | 10.4      | 8.4      | 8.8       | 8.4       | 9.0       | 9.1       | 9.1          | 8.6          | 9.1       |
| U                                | 2.2         | 2.0       | 1.5      | 1.6       | 1.4       | 1.8       | 1.6       | 1.6          | 1.8          | 1.6       |

\* All iron as Fe<sub>2</sub>O<sub>3</sub>.

\*\*Number in parentheses indicates the number of individual samples averaged.

The elements Ce, Co, Cs, Eu, Hf, Lu, Nd, Sm, Tb, Th, U, and Yb were analyzed by INAA, the others by XRF. Techniques and details of analysis are in Wunderman [1983]. Precision for all major elements is better than 1% of the amount shown, except for MgO, Na<sub>2</sub>O, and P<sub>2</sub>O<sub>5</sub>, which are about 3% of the amount shown. Precision for XRF trace elements is generally better than 5%. The INAA determinations have precisions that range from 2% (Co, Hf) to 15% (U, Nd, Tb). Analyses of standard rocks by the same methods are available from the authors on request.

believe the distribution of these deposits is consistent with their sources being directly related to the caldera (Table 6). Specifically, (1) the isopach maps of the major units generally close around the caldera, and (2) the coarsest lithic and pumice clasts in these same units are found at or near the caldera. The source vents for L and T can be shown to be near the ring fracture, based on the distribution of lithic lag breccias. The most likely source vents for the postcollapse E and J deposits are apparently the El Durazno crater (E) (Figure 2) and Laguna de Calderas (J) (Figure 2, cross section).

Volumes of airfall ash blankets were computed using a method by Rose et al. [1973], for which an interactive computer program was developed. This method offers an advantage over traditional

incremental summation techniques because it rationally estimates total volumes, not just the volume inside of measured isopachs. Thus it offers a way to estimate the volumes of fine ash that are widely scattered. All of the volumes computed have been corrected to dense rock equivalent volumes by assuming that the pyroclastic units have in situ densities of about 1.0 g/cm<sup>3</sup>, which is an average value measured in the field for Guatemalan rhyolitic tephra. The estimated volume of pyroclastic flow deposits depends on the imperfect knowledge of thicknesses and distribution of individual units in basins. The well data of Munoz et al. [1978] were of great help in this case. The pyroclastic flow volumes estimated are conservative minimum values.

Table 6 gives our best estimates of volume of

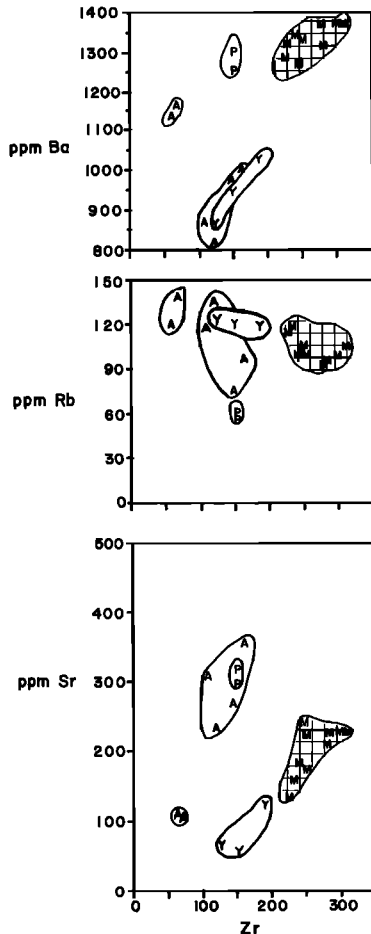


Fig. 7. Average compositions for major pyroclastic units of northern Central America. Units with sources at Amatitlan (Table 3) occupy the shaded area plotted with the symbol M. Other sources are shown as follows. A, Atitlan; Y, Ayarza; and P, Ilopango.

erupted materials in each pyroclastic unit of Amatitlan. Amatitlan has erupted at least 60–80 km<sup>3</sup> of dense rock, a figure that is typical for a caldera of just over 200 km<sup>2</sup> area [Smith, 1979].

#### Structural Geology

Amatitlan caldera lies at the intersection of two important regional faults, the Palin Shear and the Jalpatagua fault. The left-lateral Palin Shear is thought to be a transverse segment boundary between offset portions of the volcanic front [Stoiber and Carr, 1973; Carr et al., 1982]. Along the front, cones 1–7 are offset from cones 8 and 9 (Figure 1) at the location of the Shear. Physical expression of the Palin Shear itself consists of a submarine canyon on the Pacific shelf [Fisher, 1961; Eggers, 1971] and the downfaulted Guatemala City graben. Normal faults that bound the Guatemala City graben are called the Mixco (X) and Santa Catarina Pinula (C, Figure 1) faults to the west and east of the basin, respectively. The Amatitlan caldera occupies the full width of the southern part of the Guatemala City graben (Figure 1). The greatest vertical expression of the Mixco and Santa Catarina Pinula

faults occurs to the south, where the faults are tangential to the cauldron. The age of the beginning of faulting is not established, but during the 1976 Guatemalan earthquake, faults parallel and subparallel to the Mixco and Santa Catarina Pinula faults were reactivated [Plafker, 1976].

The right-lateral Jalpatagua fault zone (JFZ) follows the northern side of the volcanic chain for at least 150 km southeast of the Amatitlan volcanic center [Carr, 1974; Williams, 1960]. The fault's N65W trend is subparallel to the trench. On the east side of the cauldron the JFZ has horizontally offset several segments of the outer-boundary faults. Each displacement is about a kilometer in the right-lateral sense, with the net influence of the JFZ being spread over a zone approximately 3–6 km wide. Overall, Carr [1974] estimates the net movement of the JFZ at 9–12 km along strike, with as much as 0.5 km vertical offset.

The JFZ is expressed inside the cauldron as a longitudinal graben [Smith and Bailey, 1968] within the resurgent dome. The elongate N65W trending Lake Amatitlan is surrounded on three sides by steep cliffs of Tertiary volcanics (Figure 2). This is directly aligned with the fault's trend to the southeast (N65W), outside the cauldron (Figure 1). The downfaulted area presumably formed chiefly from tension that resulted from the influx of magma beneath, with the alignment of the resulting graben localized by the previous zone of weakness. This alignment is one of Amatitlan caldera's most striking aspects. Some other calderas have vivid linear features, particularly apical and longitudinal grabens in resurgent domes and sometimes along their walls [Smith and Bailey, 1968; Steven and Lipman, 1976]. At Timber Mountain Cauldron, younger (postcauldron collapse) regional faults do not commonly intrude beyond the "hinge line" [Christiansen et al., 1965]. From analogy with faulting at Timber Mountain, the JFZ within the cauldron block is older than the cauldron (precollapse).

Numerous domes, the E fall, and possibly the L and T eruption have vented from the area near or in the extension of the JFZ in the cauldron. Today this extension of the JFZ within the cauldron block is topographically low and contains numerous hot springs around its margins. The

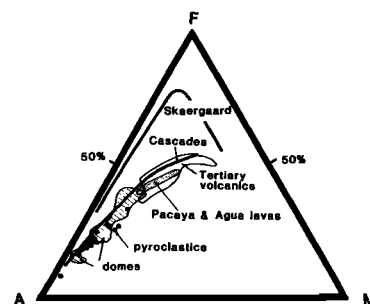


Fig. 8. AFM diagram comparing Amatitlan silicic pyroclastics (dots) to the fields of dome lavas, andesite and basalt lavas of Pacaya and Agua, and Tertiary andesite and basalt of Amatitlan Quadrangle [after Eggers, 1971]. Skaergaard and Cascades trends are shown. A = Na<sub>2</sub>O + K<sub>2</sub>O, F = FeO + 0.9 Fe<sub>2</sub>O<sub>3</sub>, M = MgO; all wt. %.

TABLE 4. Variation Analysis of Guatemalan Rhyolitic Pyroclastic Units

|    |     |     |     |     |     |     |     |     |     |     |     |     |     |     |     |
|----|-----|-----|-----|-----|-----|-----|-----|-----|-----|-----|-----|-----|-----|-----|-----|
| J2 | 100 |     |     |     |     |     |     |     |     |     |     |     |     |     |     |
| J1 | 93  | 100 |     |     |     |     |     |     |     |     |     |     |     |     |     |
| E  | 78  | 78  | 100 |     |     |     |     |     |     |     |     |     |     |     |     |
| T* | 84  | 84  | 91  | 100 |     |     |     |     |     |     |     |     |     |     |     |
| T  | 82  | 82  | 92  | 96  | 100 |     |     |     |     |     |     |     |     |     |     |
| Z5 | 78  | 77  | 91  | 89  | 89  | 100 |     |     |     |     |     |     |     |     |     |
| Z4 | 72  | 73  | 90  | 85  | 86  | 91  | 100 |     |     |     |     |     |     |     |     |
| L* | 71  | 71  | 88  | 84  | 83  | 89  | 92  | 100 |     |     |     |     |     |     |     |
| L  | 74  | 74  | 85  | 84  | 84  | 86  | 92  | 92  | 100 |     |     |     |     |     |     |
| C  | 59  | 58  | 69  | 65  | 65  | 67  | 64  | 64  | 60  | 100 |     |     |     |     |     |
| Z2 | 59  | 58  | 69  | 65  | 65  | 68  | 64  | 65  | 61  | 81  | 100 |     |     |     |     |
| PA | 82  | 84  | 75  | 79  | 78  | 73  | 70  | 68  | 72  | 58  | 57  | 100 |     |     |     |
| H* | 66  | 66  | 53  | 56  | 56  | 52  | 51  | 50  | 51  | 46  | 44  | 65  | 100 |     |     |
| H  | 70  | 69  | 58  | 62  | 62  | 56  | 56  | 53  | 57  | 53  | 49  | 68  | 83  | 100 |     |
| W  | 76  | 74  | 73  | 74  | 75  | 72  | 71  | 68  | 68  | 58  | 56  | 86  | 68  | 78  | 100 |
|    | J2  | J1  | E   | T*  | T   | Z5  | Z4  | L*  | L   | C   | Z2  | PA  | H*  | H   | W   |

The coefficient of similarity ( $\times 10^{+2}$ ) for each pair of averages is shown. Between 12 and 24 elements were used depending on available analyses for each unit. Units with an asterisk are flows, others are falls. For a description of variation analysis see Borchardt et al. [1972] and Sarna-Wojcicki et al. [1979].

escarpments along the longitudinal graben north of Lake Amatitlan are modified by scalloping.

#### Outer Boundary of Cauldron Subsidence

Cauldron faults on the outermost margins of the downdropped block, called "outer boundary faults" [Byers et al., 1976; Lipman 1974], are more easily seen than the deeply-buried ring fracture zone itself. The outer boundary faults (hereafter, OB faults) are constrained by a variety of observations that include (1) topographic expression, (2) hot spring locations, (3) the distribution of paleolacustrine sediments, and (4) gravity and resistivity data. The specific evidence for each segment was cited by Wunderman [1983].

The OB faults are constrained by and probably intersect with the Santa Catarina Pinula and Mixco faults to the east and west. In these regions the OB faults are most obvious. The OB fault's western arc is often mantled with young tephra deposits, many of which are offset by small younger faults indicating recent movement, possibly due largely to landslides. On the caldera's east wall, two segments of the OB faults can be traced along the edges of a displaced arcuate block (Figure 2). The block is offset downward with respect to the caldera wall and possibly rotated outward as well. Resulting topography of the caldera's eastern margin hence resembles stair steps. Such discontinuous arcuate steps, often showing less displacement outward, have been noted as a feature of subsidence in other cauldrons [Christiansen et al., 1977]. Displaced blocks are likely to be present elsewhere, buried by moat sediments, and thus inferred on the cross section (Figure 2). Along the west to southwest margin of the caldera the OB fault is clearly expressed by the change in relief that occurs from the steeply-sloping precaldera laharic rocks and andesite flows on the caldera wall to the flat-lying alluvium and colluvium on the moat. Southward between the well-constrained

southeast and southwest caldera walls the OB faults probably continue through Cerro Chino and the Cerro Chiquito domes on the northern flanks of Pacaya.

The northern edge of the caldera is buried and could not be delineated without the well log, seismic, electrical resistivity and qualitative gravity interpretations of Munoz et al. [1978] which reveal 200 m offset downward toward the caldera at Ojo de Agua (Figure 2, cross section). The small hills in and on the edge of the Guatemala City Basin near Ojo de Agua (Cerro Ramirez across the valley to the west, and Cerro Gordo directly adjacent and north) are probably Tertiary basement highs on the caldera rim that are now covered with tephra. The occurrence of several "circumferential" faults [Christiansen et al., 1965] along the northeast margin of the caldera also support the location of the northern OB faults as shown in Figure 2.

There are four lines of evidence that suggest both structural and magmatic resurgence of the caldera.

1. The trend of faults in the central part of the caldera differs from the regional trend [Eggers, 1971] implying different stress conditions. Many faults that trend outward from the central region appear to flare as they approach the ring fracture (Figure 2), which can be interpreted as related to resurgence. Smith and Bailey [1968, Figure 3] show that flaring of faults is common as they approach the outward edges of resurgent domes. This flaring is also seen on clay models of doming [Cloos, 1939].

2. The outstanding structural feature of the central part of the caldera is a large graben in the Lake Amatitlan area (Figure 2). The scarps bounding the graben to the north and south contain up to 300 m (north side) and 200 m (south side) of exposed precaldera rocks. The graben is strikingly similar in form to apical grabens in other calderas, especially Toba [Smith and Bailey, 1968].

3. Geophysical evidence is consistent with

TABLE 5. Average Chemical Composition of Fall Deposits From Outside of the Amatitlan Caldera

| Unit                             | Wt. %      |             |
|----------------------------------|------------|-------------|
|                                  | C<br>(n=2) | ZZ<br>(n=2) |
| SiO <sub>2</sub>                 | 68.04      | 64.7        |
| Al <sub>2</sub> O <sub>3</sub>   | 16.40      | 16.6        |
| Fe <sub>2</sub> O <sub>3</sub> * | 3.54       | 4.4         |
| MgO                              | 0.86       | 1.2         |
| CaO                              | 3.28       | 4.0         |
| Na <sub>2</sub> O                | 4.09       | 3.9         |
| K <sub>2</sub> O                 | 2.57       | 1.9         |
| TiO <sub>2</sub>                 | 0.41       | 0.40        |
| P <sub>2</sub> O <sub>5</sub>    | 0.13       | 0.16        |
| ppm                              |            |             |
| Sc                               | 6          | 6           |
| Co                               | 3.40       | 3.50        |
| Rb                               | 65         | 51          |
| Sr                               | 421        | 503         |
| Y                                | 7          | 10          |
| Zr                               | 152        | 167         |
| Cs                               | 1.50       | 1.30        |
| Ba                               | 904        | 958         |
| La                               | 26         | 22          |
| Ce                               | 64         | 45          |
| Nd                               | 19         | 15          |
| Sm                               | 3.60       | 4.60        |
| Eu                               | 1.14       | 1.40        |
| Tb                               | 0.45       | 0.87        |
| Yb                               | 1.40       | 1.90        |
| Lu                               | 0.23       | 0.29        |
| Hf                               | 4          | 4           |
| Pb                               | 17         | 21          |
| Th                               | 4.00       | 3.55        |
| U                                | 0.43       | 0.64        |

See Table 3 for explanation of footnotes.

resurgence. Resistivity, seismic, and water well information compiled by Munoz et al. [1978] within the north-central area of the caldera indicates the buried surface of the precaldern rocks tilts out away from the caldera's center (Figure 2, cross section). However, Eggers [1971, and personal communication] cites horizontal attitudes and uniform present-day elevations of lake sediment deposits in and around the caldera as possible evidence against resurgence. This evidence is hard to evaluate since stratigraphic position, correlation, and original depositional geometry of the sediments he refers to are unknown. Also lake sediments may have once been present on now uplifted portions of the resurgence dome and subsequently removed by erosion.

4. The location of relatively recent (post-T) volcanic activity, including many silicic domes and the widespread E fall (see above), has taken place in the central part of the caldera near the graben. This is consistent with magma resurgence in the central part of the caldera.

Evidence for continuing resurgence is provided by the young domes in the village of Amatitlan and

near Villa Nueva and young Amatitlan plinian airfalls such as J3, J2, and J1. The dome near Villa Nueva must be between 40 and 84 kyr, based on its relationship to dated pyroclastic units. The falls are younger than 23,000 years BP. Seismic and thermal activity is also consistent with continuing resurgence (see below).

#### History and Present State of the Amatitlan Caldera

The outward dipping Tertiary rocks in the vicinity of the cauldron are evidence of a past topographic high, thought to have been a constructional feature built by volcanic products and perhaps by structural doming. Highs such as this may also be interpreted as a result of precollapse tumescence [Smith and Bailey, 1968]. After magma ascent, the magma presumably resided in a high-level chamber for some unspecified length of time, long enough to produce chemical zonations in the magma [Smith, 1979; Hildreth, 1979].

The L eruption is the first documented pyroclastic eruption from Amatitlan (Figure 9). It is estimated to be at least 18 km<sup>3</sup> (DRE), large enough to cause significant caldera collapse. Lake sediments help define the caldera which formed after eruption of L. A second major eruption, T, at about 0.24 Ma. produced additional caldera collapse. It's estimated minimum volume is 17 km<sup>3</sup> (DRE). After this, surface resurgence certainly occurred (Figure 9).

With resurgence, the emplacement of at least 14 dacite to andesite domes south and west of the present Lake Amatitlan began [Eggers, 1971] and continued. The extra-caldern C eruption occurred following the onset of resurgence. Agua's volcanic activity commenced after the C eruption since cinders on its western flanks are interbedded with post-C fall material. Next the caldera was breached to the south. The E eruption followed.

The J eruptions are the youngest near-source pyroclastics at Amatitlan. Currently, hot spring and seismic activity persist at Amatitlan, indicating the continued presence of magma at depth. Further eruptions are likely, especially plinian fall and dome eruptions on the ring fracture. The evolution of Amatitlan appears to correspond well to the model of Smith and Bailey [1968]; the stage of activity is then somewhere between stage V (resurgent doming) and stage VI (major ring-fracture volcanism). Peculiarities in Amatitlan's history include development of the unusually large longitudinal graben, burial of the caldera's northern boundary by sediments, and evolution of the Pacaya complex on its southern edge [see Eggers, 1971].

The age of "ancestral Pacaya", a Quaternary stratovolcano on which the modern Pacaya is built, cannot be well constrained. It may predate the L eruption, but it was apparently influenced by the ring-fracture system. The modern Pacaya cone is probably younger than all of the Amatitlan pyroclastics [Eggers, 1971].

One of the current features of Amatitlan is the cluster of small earthquake epicenters in the northern resurgent dome in the ring-fracture region. The starred pattern of Figure 1 shows the distribution of earthquakes for May 1976. This

TABLE 6. Volumes and Sources of Amatitlan Pyroclastic Deposits

| Tephra   | Source Vent Locations  | Minimum Volume DRE (km <sup>3</sup> )* |
|--|--|--|
| J3 fall  | Lagunas Calderas, Pacaya complex or Caldera's dome   | 0.05                                   |
| J2 fall  | complex? Each may have a separate vent.  | 0.05                                   |
| J1 fall  |  | 0.1                                    |
| E fall   | El Durazno Crater  | 2.5                                    |
| C fall   | Sabana Grande region?  | 0.8                                    |
| T ash flow   | Within Caldera, probably along now-buried ring fractures and/or longitudinal graben (western central part of Caldera?) | 13 (outflow)                           |
| T fall   |  | 4.0                                    |
| Z5 fall  | Near U.N. Park   | 0.06                                   |
| Z4 fall  | Near U.N. Park, probably in or near ancestral Caldera lake   | 0.08                                   |
| Z2 fall  | Outside of Caldera; Sabana Grande region?  | ? negligible                           |
| L ash flow   | Within Caldera, probably along now-buried ring fractures   | 12 (outflow)                           |
| L fall   | (eastern side of Caldera?)   | 6.0                                    |
| Amatitlan units in Nueva Santa Rosa region; identification of exact unit is uncertain (likely to be mainly L, T, and E(?) units) |  |  |
|  | Ash flows  | 10                                     |
|  | Falls  | 5                                      |
| Amatitlan subtotal   |  | 53                                     |
| Additional intracaldera volume of ash (see text; mainly ash flows (?))   |  | 8-33(?)                                |
| Amatitlan total (minimum, rough estimate)  |  | 60-80                                  |

\*Conversion used for dense rock equivalent (DRE) to actual volume is 2.2.

cluster is persistent, though sometimes diminished, in the time interval for which published seismic data exists, March 1, 1975 to June 1976 [Harlow and White, 1980; White and Harlow, 1979, 1980]. The cluster does appear during other more recent periods as well [R. White, personal communication]. Significance of the earthquakes is still unclear, but one interpretation is that they are caused by surfaceward intrusion of a tongue of magma in a situation somewhat analogous to Long Valley, California. Alternatively, the clustering of seismic events seen in Figure 1 could represent readjustment after the February 1976 Guatemala earthquake [Plafker, 1976]. This does not explain why earthquakes both preceded and continued long after the major quake [Harlow and White, 1980; White and Harlow, 1980]. The young dome at Villa Nueva is suggestive of the presence of still molten magma at depth. More than a million people live within 20 km of Amatitlan, suggesting the importance of further studies on hazard-related topics. These should include specific study of the cluster of epicenters, confirmation of the

rate of resurgence using geodetic techniques, hot spring temperature and chemistry, fission track dating of pyroclastic and dome eruptive units, and possibly geophysical research aimed at identifying the presence of molten magma near the surface.

#### Conclusions

Reinterpretation of existing geologic and geophysical work combined with new field work and extensive laboratory studies has resulted in the recognition of a 14 x 16 km collapse caldera located at the southern end of the Guatemala City graben, south of Guatemala City. The proximity of this feature to a major city makes its recognition extremely important because of the implications for volcanic hazards. The essential evidence for the caldera are (1) numerous large pyroclastic deposits with a local source, (2) a prominent gravity low, (3) the topographic and structural features associated with other calderas, such as arcuate faults, resurgent domes, volcanic domes and circumferential faults, (4) hot spring and fumarolic activity, (5) seismic and geological evidence of active resurgence, and (6)

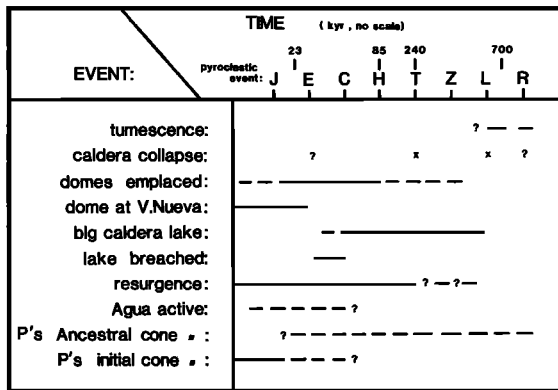


Fig. 9. Inferred timing and duration of cauldron-related events and processes at Amatitlan. Crosses denote a well constrained event, solid lines used where the timing is relatively well documented, and dashes where less well documented. Question marks mean little is known about the timing of an event. The most closely time constrained events include the two caldera collapses, the existence of a widespread lake and the timing of the lake's breaching, and the relatively recent intrusion of a dacite dome in the northern part of the caldera.

lithological changes in sedimentary rocks at the caldera boundary that outline a former caldera lake.

The caldera has produced at least nine significant pyroclastic eruptions over a time period of about 300,000 years. It must be considered active and likely to erupt again. Respose intervals between eruptions are long, however. Observational data should be collected in certain areas. Such data may permit recognition of the time and place of renewed volcanic activity. Extrapolating from the most recent past record, the most likely type of activity may be plinian or phreatoplinian airfall eruption or dome extrusion in the vicinity of Lake Amatitlan or in the northern part of the caldera.

Modern calderas are not necessarily spectacular landforms, but may be (on the surface) very subtle features, requiring a battery of techniques for correct interpretation. There are probably many more examples of unidentified active calderas in populous areas. We hope our experience at Amatitlan will help others recognize them.

**Acknowledgements.** Funding for this work came from the National Science Foundation, through grants EAR 78-01180 and EAR 82-05605. The Guatemalan government, through the Instituto Geografico Nacional and Oscar D. Salazar, provided logistical help, an excellent base map, and aerial photographs. We wish to thank Al Eggers and John Wolff for critical reviews; Bob Christiansen, Charlie Bacon, Don Noble, Ted Bornhorst, Randy White, and Dave Harlow for discussion; and Jimmy Diehl for paleomagnetic determination of an oriented sample.

#### References

Bonis, S.B., O. Bohnenberger, and G. Dengo, Mapa Geologico de la Republica de Guatemala, scale

- 1:500,000, Instituto Geografico Nacional de Guatemala, 1970.
- Borchardt, G.A., P.J. Aruscavage, and H.T. Millard, Jr., Correlation of the Bishop ash, a Pleistocene marker bed, using instrumental neutron activation analysis, *J. Sediment. Petrol.*, **1**, 301-3206, 1972.
- Brown, R.H., A.L. Lamarre, R.A. Lamarre, and T. A. Loucks, Geology of the eastern portion of the San Jose Pinula Quadrangle, Guatemala, 102 pp., Dartmouth Coll., Hanover, N. H., 1971.
- Byers, F.M., Jr., W.J. Carr, P.P. Orkild, W.D. Quinlivan, and K.A. Sargent, Volcanic suites and related cauldrons of Timber Mountain-Oasis Valley caldera complex, southern Nevada, *U.S. Geol. Surv. Prof. Pap.*, **919**, 70 pp., 1976.
- Carr, M.J., Tectonics of the Pacific margin of northern Central America, Ph.D. thesis, Dartmouth Coll., Hanover, N.H., 1974.
- Carr, M.J., R.E. Cox, J.C. Knapp, C.C. Pineo, and J.J. Ross, Geology of the southwest portion of the San Jose Pinula Quadrangle, Guatemala, thesis, 102 pp., Dartmouth Coll., Hanover, N.H., 1969.
- Carr, M.J., W.I. Rose, Jr., and R. Stoiber, Volcanism in Central America, in *Orogenic Andesites and Related Rocks*, edited by R.S. Thorpe, pp. 149-166, John Wiley, New York, 1982.
- Christiansen, R.L., P.W. Lipman, P.P. Orkild, and F.B. Byers, Structure of the Timber Mountain caldera, southern Nevada, and its relation to basin-range structure, *U.S. Geol. Surv. Prof. Pap.*, **525-B**, 43-48, 1965.
- Christiansen, R.L., P.W. Lipman, W.J. Carr, F.M. Byers, Jr., P.P. Orkild, and K.A. Sargent, Timber Mountain-Oasis Valley caldera complex of southern Nevada, *Geol. Soc. Am. Bull.*, **88**, 943-959, 1977.
- Cloos, H., Hebung-Spaltung-Vulkanismus, *Geol. Rund. Schau*, **30**, 405-528, 1939.
- Drexler, J.W., Geochemical correlations of Pleistocene rhyolitic ashes in Guatemala with deep-sea ash layers of the Gulf of Mexico and equatorial Pacific, M.S. thesis, Mich. Technol. Univ., Houghton, 1978.
- Drexler, J.W., W.I. Rose, Jr., R.S.J. Sparks, and M.T. Ledbetter, The Los Chocoyos Ash: Quaternary stratigraphic marker in Middle America and three ocean basins, *Quaternary Res.*, **13**, 373-391, 1979.
- Durgin, D., G.B. Malone, and P.C. Vikre, Geology of the northwest portion of the San Jose Pinula Quadrangle, Guatemala, Dartmouth Coll., Hanover, N.H., 1970.
- Eggers, A.A., The geology and petrology of the Amatitlan Quadrangle, Guatemala, Ph.D. thesis, Dartmouth Coll., Hanover, N.H., 1971.
- Eggers, A.A., Mapa Geologico de Amatitlan, Hoja 2059116, Instituto Geografico Nacional de Guatemala, 1975.
- Fisher, R.L., Middle America Trench: Topography and structure, *Geol. Soc. Am. Bull.*, **72**, 703-720, 1961.
- Hahn, G.A., Interbasin geochemical correlation of genetically related rhyolitic ash-flow and airfall tuffs, central and

- western Guatemala, M.S. thesis, Mich. Technol. Univ., Houghton, 1976.
- Harlow, D.H., and R.A. White, Preliminary catalog of seismicity prior to the Guatemalan earthquake of February 4, 1976, from the area between Guatemala City and Lake Atitlan (March 1975-February 1976), U.S. Geol. Surv. Open File Rep., 80-60, 24 pp., 1980.
- Hildreth, W., The Bishop Tuff: Evidence for the origin of compositional zonation in silicic magma chambers, Geol. Soc. Am. Spec. Pap., 180, 43-75, 1979.
- Koch, A., Stratigraphy, petrology and distribution of Quaternary pumice deposits of the San Cristobal group, Guatemala City area, Guatemala, Ph.D. thesis, Univ. of Wash., Seattle, 1970.
- Koch, A., and H. McLean, Pleistocene tephra and ash-flow deposits in the volcanic highlands of Guatemala, Geol. Soc. Am. Bull., 86, 529-541, 1975.
- Koch, A., and H. McLean, Mapa Geologica de Guatemala, Hoja 2059 IG, Instituto Geografico Nacional de Guatemala, 1977.
- Ledbetter, M.T., Tephrochronology of marine tephra adjacent Central America, Geology, in press, 1983.
- Lipman, P.W., Geologic map of Platoro Caldera area, southwestern San Juan Mountains, southwestern Colorado, U.S. Geol. Surv. Misc. Inv. Ser. Map I-828, 1974.
- McLean, H., Stratigraphy, mineralogy and distribution of the Sumpango Group pumice deposits in the volcanic highlands of Guatemala, Ph.D. thesis, Univ. of Wash. Seattle, 1970.
- Munoz, C.E., E. Velasquez, V.R. Aragon, and B. De Morales, Informe Final, Estudio de aguas subterranas en el valle de la Ciudad de Guatemala, Ministerio de Comunicaciones y Obras Publicas, Guatemala, 78.
- Newhall, C.G., 1981, Geology of the Lake Atitlan area, Guatemala, Ph.D. thesis, Dartmouth Coll., 364 p.
- Peterson, P.S., Tephra of the Laguna de Ayarza calderas of southeastern Guatemala and its correlation to units of the Guatemala Highlands, M.S. thesis, Mich. Technol. Univ., Houghton, 1980.
- Plafker, G., Tectonic aspects of the Guatemala earthquake of 4 February 1976, Science, 193(4259), 1201-1208, 1976.
- Reynolds, J.J., Tertiary volcanic stratigraphy of northern Central America, M.S. thesis, 89 pp., Dartmouth Coll., Hanover, N.H., 1977.
- Reynolds, J.J., Late tertiary volcanic stratigraphy of northern Central America, Bull. Volcanol., 43(3), 601-608, 1980.
- Rose, W.I., Jr., Notes on fumaroles and recent volcanic activity on Volcan Pacaya, Instituto Geographico Nacional (Guatemala), Geol. Bull., 4, 31-33, 1967.
- Rose, W.I., Jr., S. Bonis, R.E. Stoiber, M. Keller, and R. Bickford, Studies of volcanic ash from two recent Central American eruptions, Bull. Volcanol., 37, 338-354, 1973.
- Rose, W.I., Jr., G.A. Hahn, J.W. Drexler, M.L. Malinconico, P.S. Peterson, and R.L. Wunderman, Quaternary tephra of northern Central America, in Tephra Studies as an Aid in Quaternary Research, edited by S. Self and R.S.J. Sparks, D. Reidel, Hingham, Mass., 1981.
- Sarna-Wojcicki, A.M., H.W. Bowman, and P.C. Russel, Chemical correlation of some Cenozoic tuffs of northern and central California by neutron activation analysis of glass and comparison with X-ray fluorescence analysis, U.S. Geol. Surv. Prof. Pap., 1147, 1979.
- Smith, R.L., Ash-flow magmatism, Ash-flow Tuffs, Geol. Soc. Amer. Spec. Pap., 180, 5-29, 1979.
- Smith, R.L., and R.A. Bailey, Resurgent cauldrons, Geol. Soc. Am. Mem., 116, 613-661, 1968.
- Steven, T.A., and P.W. Lipman, Calderas of the San Juan volcanic field, southwestern Colorado, U.S. Geol. Surv. Pap., 958, 35 pp., 1976.
- Stoiber, R.E., and M.J. Carr, Quaternary volcanic and tectonic segmentation of Central America, Bull. Volcanol., 37, 304-325, 1973.
- White, R.A., and D.H. Harlow, Preliminary catalog of aftershocks of the Guatemala earthquake of February 4, 1976, from the area between Guatemala City and Lake Atitlan (February-June 1976), U.S. Geol. Surv. Open File Rep., 79-864, 60 pp., 1979.
- White, R.A., and D.H. Harlow, Preliminary catalog of seismicity from south-central Guatemala (July-December 1976), U.S. Geol. Surv. Open File Rep., 80-83, 1980.
- Williams, H., Volcanic history of the Guatemalan Highlands, Univ. Calif. Berkeley Publ. in Geol. Sci., 38, 86, 1960.
- Wunderman, R.L., Amatitlan, an active resurgent caldera immediately south of Guatemala City, Guatemala, M.S. thesis, 192 pp., Mich. Technol. Univ., Houghton, 1983.

W.I. Rose and R.L. Wunderman, Department of Geology and Geological Engineering, Michigan Technological University, Houghton, MI 49931

(Received September 7, 1983;  
revised January 6, 1984;  
accepted March 23, 1984.)